(Received 2 August 2024, Accepted 10 September 2024, Scheduled 24 September 2024)

A Compact Four Port MIMO Antenna for n261 Millimeter Wave Band Applications

Reena Aggarwal[1], Ajay Roy[1], and Rajeev Kumar[2, *]

[1] School of Electronics and Electrical Engineering, Lovely Professional University, Punjab, India
[2] Chitkara University Institute of Engineering and Technology, Chitkara University, Punjab, India

ABSTRACT: This article introduces a compact design for a four-element MIMO antenna for millimeter-wave (mmWave) communications for specifically n261 band having range from 27.5 GHz to 28.35 GHz with a bandwidth of 850 MHz. The single antenna structure uses a rectangular patch having four diamond-shaped slots in the feed-plane. On the ground plane, a dumbbell-shaped slot is positioned below the rectangular patch. A Rogers RT/Duroid 5880 substrate with ultra-thin thickness is used in this design. The optimized design for four-port MIMO antenna has small size with dimensions of 20 mm $\times$ 19 mm $\times$ 0.254 mm. The MIMO parameters such ECC is less than 0.011, and DG is greater than 9.90 dB in the mentioned bands, which are within tolerance limits. The isolation between neighbouring MIMO elements is also less than -19.5 dB.

1. INTRODUCTION

In microstrip antennas, defected ground surface (DGS) is a popular technique which refers to slots or defects etched out in ground plane. With the placement of a simple structural DGS design in ground plane, performance characteristics like gain, bandwidth, and cross-polarisation can be enhanced [1]. In multiple-input multiple-output (MIMO), DGS can also be utilized for reducing coupling of antenna elements with each other. In [2], a trimmed ground plane is used to enhance the bandwidth with one-element antenna resonating in range 26–30 GHz with 4 GHz bandwidth, and in MIMO setup with four elements, 24 dB isolation was achieved. Similarly, in [3], DGS implementation generates a wideband output of 4.1 GHz in range 25.5–29.6 GHz with isolation below 10 dB between radiating elements. In another design, authors in [4] attain an isolation of $>$ 25 dB between MIMO elements by utilizing a zig-zag shaped slot to enhance mutual isolation. DGS can also be used to introduce notch-band characteristics; for example in [5], a simplified composite right/left-handed (SCRLH) resonator has been used to introduce notch-bands in an ultra-wide bandpass filter. Similarly, in [6], notch-band has been introduced by introducing a folded stepped impedance resonator (SIR).

Among various DGS designs available in literature, "dumbbell" shaped DGS (DB-DGS) has attracted lot of interest [7–9]. DB-DGS can also be used as stopband filters [10], sensors [11], common-mode noise suppression [12], etc. In this paper, we have utilized dumbbell shaped resonator which is placed in ground plane to improve characteristics of the antenna radiating in n261 band.

Similar to other mmWave bands, n261 is also considered for short range, low latency, and high data rate applications. n261 which is the subset of n257 ranges from 27.5 GHz to 28.35 GHz with a bandwidth of 850 MHz. In [13], a Vivaldi slot antenna for mmWave Ka band suitable for n257 and n261 band applications and centered at 28 GHz is proposed. For human body-centric networks applications, another 8-element MIMO antenna [14] radiating in n261 band which is centered at 27 GHz and has bandwidth of 2 GHz is proposed. To achieve adequate isolation between adjacent radiating elements, ground plane is etched with a wall of slots. In [15], a 4-port MIMO antenna supporting multiple-bands for on-body is proposed having wideband characteristics in range 8.31–36.14 GHz.

A 1×4 array patch antenna with coplanar feed covering n257/n258/n261 band (24.25–29.5 GHz) is proposed in [16] for 5G NR radio. Antenna array elements are separated by 6 mm (~ 0.5 lambda at 25 GHz), giving a small antenna size of 26 mm $\times$ 5 mm for 1×4 array. In another design, a 2-element MIMO antenna using rectangular slot for creating defect in both the feed-patch and ground is proposed in [17] for 28 GHz applications. The design provides good isolation and gain.

The proposed antenna design is narrowband which is specifically designed for n261 band applications. The n261 band ranges from 27.5 GHz to 28.35 GHz with a bandwidth of 850 MHz. The overall structural dimensions achieved for the proposed 4-port MIMO antenna are $20 \times 19 \times 0.254$ mm^3 which to the best of the authors' knowledge is smaller than other structures proposed in literature for this band. Additionally, the proposed antenna is narrowband typically covering only n261 band meant for applications requiring the use of this specific band. Table 1 shows a comparison with some of the recent papers meant for n261 band applications.

In Section 2, we discuss the design aspect of the proposed antenna. In Section 3, we describe the details of how the stepwise development of antenna design was undertaken. Section 4

* Corresponding author: Rajeev Kumar (rajeev.kumar@chitkara.edu.in).

TABLE 1. Comparison between our work and other related articles.

Ref.	Year	Centered Freq/Band	Band Width (GHz)	Structure Shape	Size (mm)	No. of MIMO Ant.	DG (dB)	Peak Gain (dBi)	ECC	Min Isolation (dB)
[13]	2024	28 GHz/n257, n261	4.87	Slotted vivaldi meander	$50 \times 20 \times 1.6$	1	na	6.65	NA	na
[14]	2024	27 GHz (Medical)/n261	2	T-shaped patch	$22 \times 17 \times 0.5$ (Single element)	8	9.97	4.64 dB	0.005	-22 dB
[15]	2023	FR2, K, Ka, Ku, X (8.31 GHz–36.14 GHz)	27.83	Slotted Hexagonal patch	$20 \times 20 \times 0.254$	4	> 9.99	7.17	< 0.01	na
[16]	2022	n257/n258/n261 (23–30.5 GHz)	7.5	coplanar feed patch	$26 \times 5 \times 1.524$	4	na	9.76	na	> -16 dB
[17]	2021	28 GHz	-	Rectangular slot in feed & ground plane	$30 \times 15 \times 0.25$	2	9.99	5.4	< 0.008	-35
[20]	2020	28 GHz (26.71–28.91 GHz)	2.2	Metamaterial DRA	$20 \times 40 \times 1.6$	4	na	7.0	0.02	-29.34
[21]	2017	28 GHz	1.75	Cylindrical dielectric resonator (cDRA) based MIMO	$40 \times 10 \times 1.16$	2	na	7.0	< 0.4	-25
[22]	2021	28 GHz	1.5	Feedline with 3-circular shaped rings	$30 \times 30 \times 0.78$	4	9.87	6.1	< 0.16	-29
Our Work	2024	28 GHz/n261	0.85 (n261 exclusive)	Slotted Patch with ground DGS	$20 \times 19 \times 0.254$	4	9.90	5.84	< 0.011	-19.5

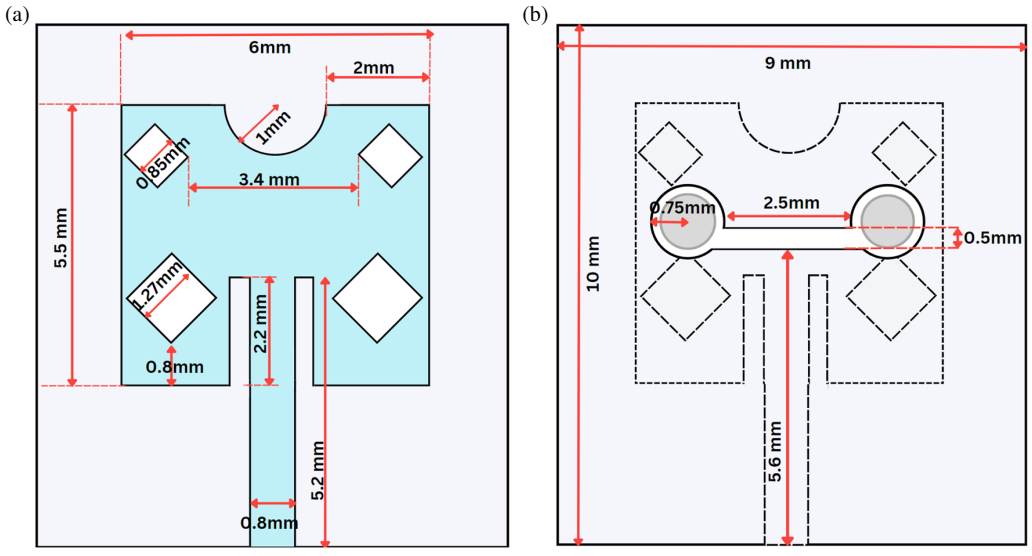

FIGURE 1. Design structure of single element. (a) Feed plane, (b) ground plane.

deals with how dimensional parameters of antenna are altered to get optimized results.

2. ANTENNA DESIGN

The antenna design is compact, simple, and symmetrical but requires precise alignment of ground and feed-plane. A Roger RTduroid 5880 substrate of 0.254 mm thickness is used in this design.

2.1. Feed Plane

The design of the antenna, shown in Figure 1(a), consists of a 6 mm $\times$ 5.5 mm rectangular patch which is fed by a 0.8 mm

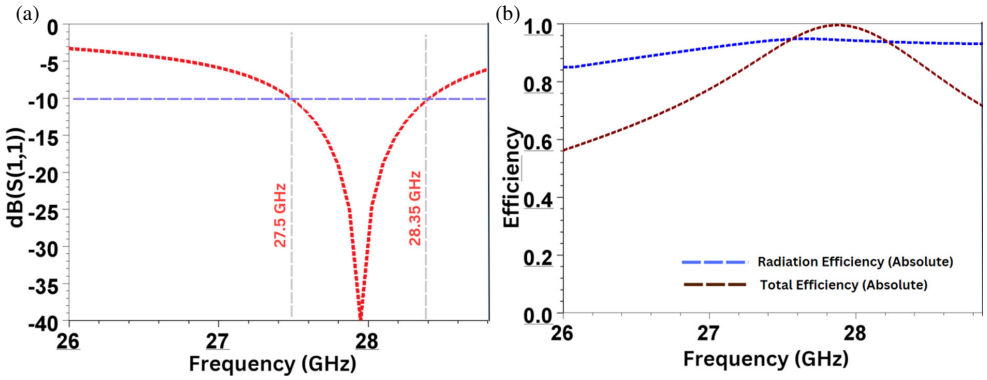

FIGURE 2. (a) S_{11}. (b) Radiation & total efficiency.

wide feed-line. Three types of slots are carved-out from the rectangular patch. Firstly, a semicircular slot of 1 mm radius is etched from the top middle part of the rectangular patch. Second types of slots are four diamond shaped slots. Two diamond-slots placed below are $1.27\,\text{mm} \times 1.27\,\text{mm}$, and those placed above are smaller with dimensions $0.85\,\text{mm} \times 0.85\,\text{mm}$. The third set of slots are $2.2\,\text{mm} \times 0.4\,\text{mm}$ slots, each placed at both sides of the feed line.

2.2. Ground Plane

The ground plane, shown in Figure 1(b), consists of two circular slots of 0.75 mm radius which are connected with each other by using a $2.5\,\text{mm} \times 0.5\,\text{mm}$ rectangular slot. With respect to the centre line of rectangular slot, the centres of the circles are displaced upwards by 0.6 mm to get the desired results. The combined shape of the slot looks like "dumbbell". To further improve the reflection coefficient, another circular patch of 0.74 mm is placed within both the circular slots.

As given in Figure 2(a), the simulated result of reflection coefficient (S_{11}) is depicted for a single element antenna. It can be seen that as per the reference of -10 dB impedance bandwidth, there is a good return loss from frequency 27.50 to 28.35 GHz which yields a bandwidth of 850 MHz. This completely covers n261 band frequency of FR2. Similarly, Figure 2(b) depicts the response of simulated absolute values for total & radiation efficiency. The achieved response of radiation efficiency is > 0.93 for the wanted frequency range. The value for total efficiency varies within the range of 0.85–0.98.

3. EVOLUTION

Although the final structural design is achieved after numerous iterations of optimization process, for an easy understanding, we have summarized the evolution process in simple four steps. To achieve the final design, in each step variations in dimension size and shape of structural parts are carried out. The step-wise summary of the activity is given below:

Step-1: Initially, as depicted in Figure 3(a), a simple structure is created with a rectangular patch which is fed by a feed line. First, the width W and length L of the rectangular patch are calculated by below mentioned standard equations [18, 19]

$$W = \frac{c}{2f_r}\sqrt{\frac{2}{\varepsilon+1}}, \quad L = \frac{c}{2f_r\sqrt{\varepsilon_r}} - 2\Delta L$$

where W is the width of the patch, and L is the length of the patch.

ε_r is the relative dielectric constant of the substrate, and h is the height of the substrate. The effective dielectric constant ε_{reff} and ΔL are calculated by following formula

$$\varepsilon_{reff} = \frac{\varepsilon+1}{2} + \frac{\varepsilon-1}{2}\left(1+12\,\frac{h}{W}\right)^{-1/2},$$

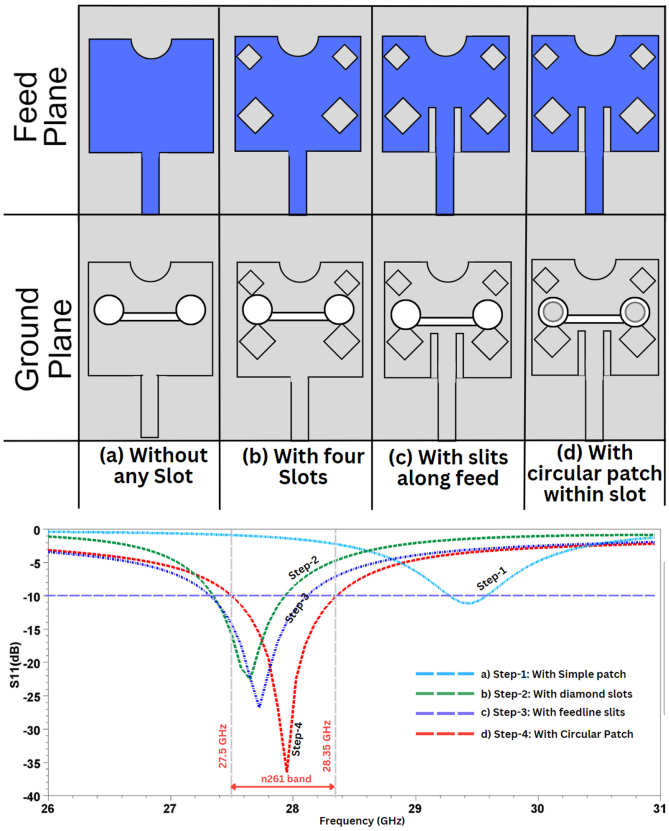

FIGURE 3. Step-wise antenna design.

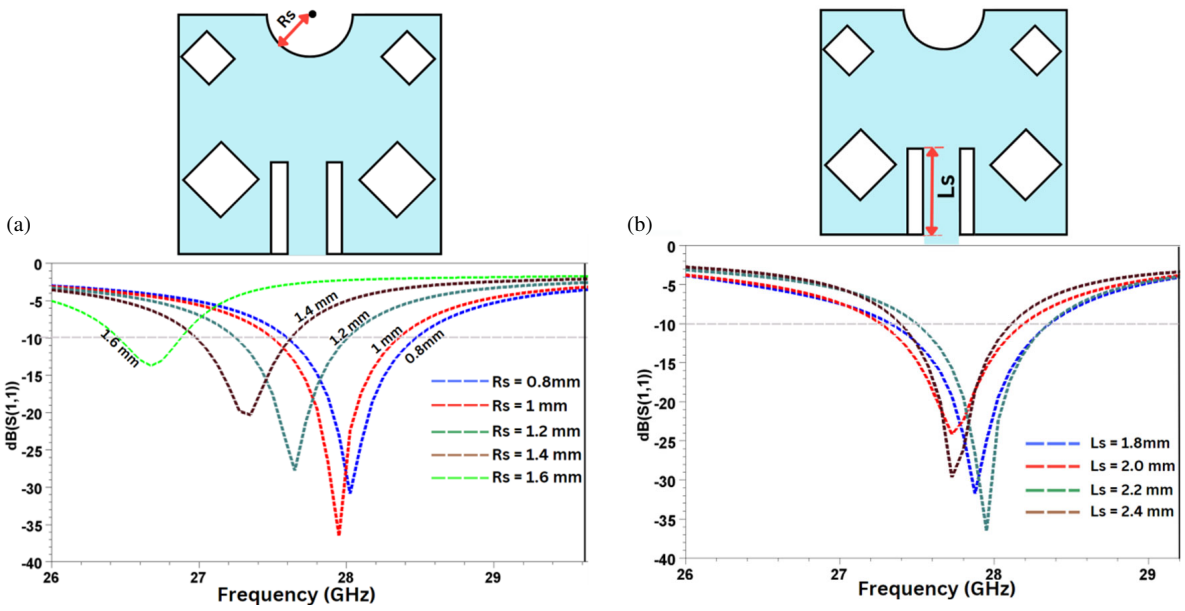

FIGURE 4. Optimization with (a) variation in Rs, (b) variation in Ls.

$$\frac{L}{h} = 0.412\,\frac{(\varepsilon_r + 0.3)\left(\frac{W}{h} + 0.264\right)}{(\varepsilon_r - 0.258)\left(\frac{W}{h} + 0.8\right)}$$

Subsequently, on the ground plane two circular shapes are etched out which are joined by a horizontal bar. The structure is optimized, but it resonates at around 29.43 GHz with narrow bandwidth and poor return loss.

Step-2: Four diamond-shaped structures are etched out in the feed plane as shown in Figure 3(b). The structure is seen to resonate 27.64 GHz with much better bandwidth. However, we require the antenna for n261 (27.5–28.35 GHz). So, further fine-tuning is required.

Step-3: Two stubs are removed from both sides of the feed line as shown in Figure 3(c), which substantially improves the return loss.

Step-4: In this step, a circular patch is placed within the etched-out circles in ground plane as shown in Figure 3(d). The return loss is further improved, and antenna exactly resonates with the bandwidth of 27.5–28.35 GHz.

4. PARAMETRIC ANALYSIS

Optimization task is performed by altering the dimensions of structures in the antenna design. Different dimensional parameters have different levels of impact on the radiation characteristics. In this section, we will discuss those dimensional parameters of the design which have significant effect on the antenna characteristics.

4.1. Radius of Feed-Plane Circle (Rs)

The change in the radius of the circular slot placed on upper position of rectangular patch changes the radiating frequency. As shown in Figure 4(a), with the increase in radius, the effective length is also increased which causes the frequency to shift downwards. The structure can be made to resonate at other frequencies also by altering Rs. However, the return loss needs to be optimized by other structural changes. For n261 band, optimum results are generated at $Rs = 1$ mm.

4.2. Length of Slit along the Feed-Line (Ls)

The return loss is improved significantly with the change of length of the slit placed on both sides of feed-line. As can be seen from Figure 4(b), the return loss is better for $Ls = 2.2$ mm.

4.3. Radius of Circular Slots in Ground Plane (Rc)

By the variation of radius of two circular slots placed in ground plane, resonant frequency can be altered as shown in Figure 5(a). Since in this paper we are interested in n261 band, our requirement is satisfied by using $Rc = 0.75$ mm.

4.4. Width of Rectangular Slot in Ground Plane (Wid)

By altering the width of the rectangular slot, there is a sharp change in the resonating frequency. In addition, the return loss is also good for resonating frequencies. In this structure, the resonant cavity is formed by combined slot formed by both the circular slots and their inter-connecting rectangular slot making a shape of dumbbell. The resonant frequency is determined by the effective length created by the combined slot dimensions in ground plane. Consequently, any change in radius (Rc) and width (Wid) causes change in the effective length which leads to sharp change in the frequency as shown in Figures 5(a) and (b). This is further corroborated when the analysis of induced current is done in Section 6.4, where large current gets induced at resonant frequency at the inner edge of both the circles and connecting rectangle (dumbbell).

Based on the above discussion, we can clearly infer that the proposed structure can be made to resonate over wide range of frequencies with minor alteration of dimensional parameters.

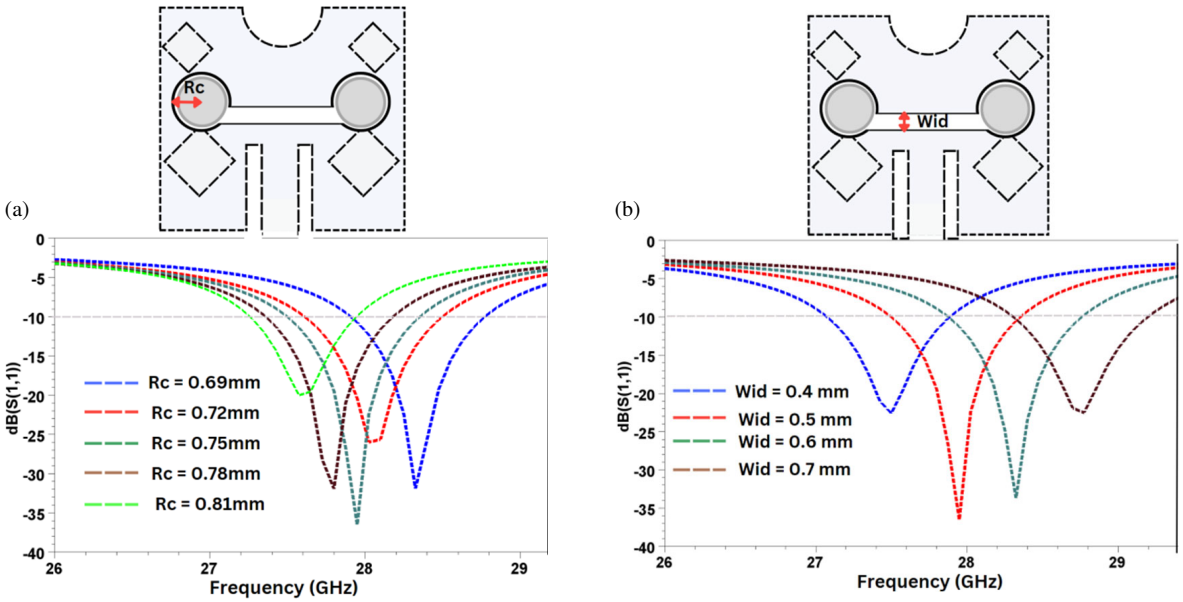

FIGURE 5. Optimization with (a) variation in Rc, (b) variation in Wid.

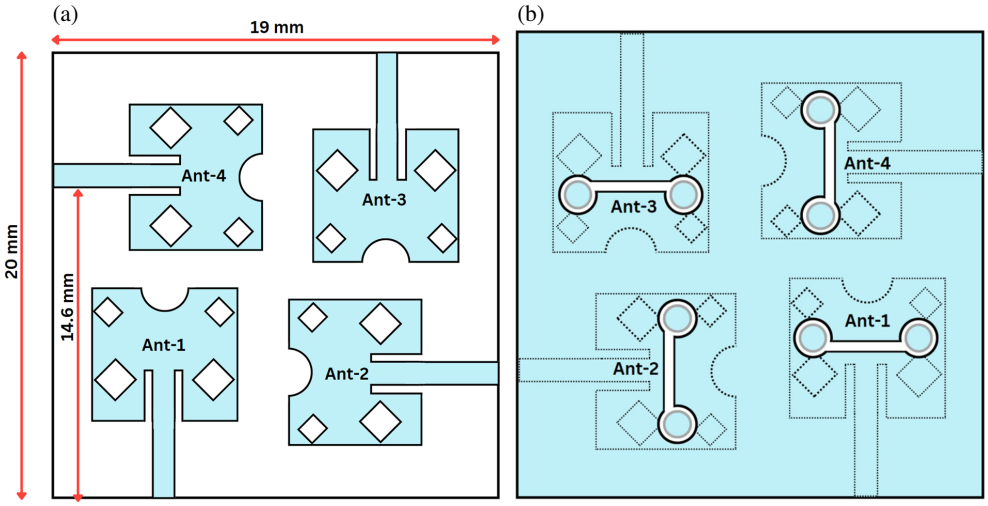

FIGURE 6. MIMO antenna design. (a) Feed plane (top view), (b) ground plane (bottom view).

5. MIMO ANTENNA DESIGN

The single-element antenna design described above is used to develop a MIMO antenna with a four-element design so as to attain both the high channel capacity and data rates in mmWave frequency. As depicted in Figure 6(a), our proposed design for MIMO antenna has four antennas placed in feed-plane in polarization diversity configuration. The plane on the other side, shown in Figure 6(b), has a common ground plane having separate dumbbell shaped slots corresponding to each element. The optimized size for the proposed MIMO antenna structure is 20 mm × 19 mm.

6. RESULTS AND DISCUSSION

The fabricated prototype of the proposed MIMO antenna is as shown in Figure 7.

6.1. S-Parameters

Simulated results with all four radiating MIMO antennas are as shown in Figure 8. As can be seen from Figure 8(a), there is a minor shift in the operating frequency as compared to a single-element antenna. Antenna-1 radiates between 27.49–28.39 GHz, antenna-2 between 27.50–28.36 GHz, antenna-3 between 27.50–28.37 GHz, and antenna-4 between 27.50–28.42 GHz. As seen from Figure 8(b), adjacent antennas isolation for the desired bandwidth is achieved to be less than −20 dB. In this design, the mutual isolation is achieved without the use of any additional decoupling structure. Another method which is generally used in increasing the mutual isolation is by increasing the separation between the elements, but this method increases the overall dimensions of the antenna. In our design, the distance between the adjacent elements has been optimally

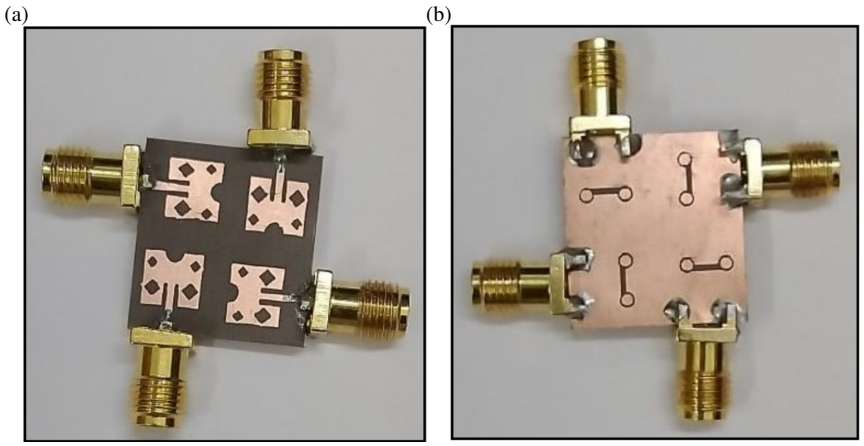

FIGURE 7. Fabricated design of proposed MIMO antenna. (a) Feed plane, (b) ground plane.

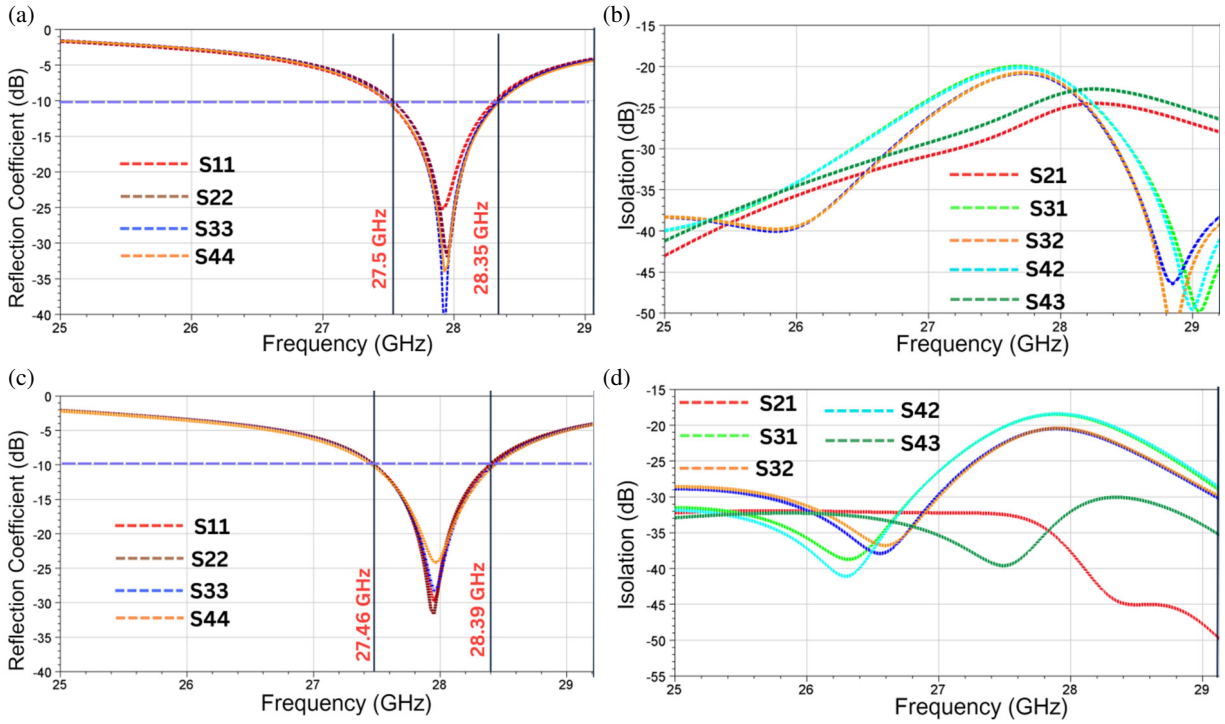

FIGURE 8. (a) Simulated reflection coefficient. (b) Simulated isolation. (c) Measured reflection coefficient. (d) Measured isolation.

placed to achieve adequate mutual decoupling. Moreover, the MIMO antennas are placed at orthogonal position with each other so as to achieve low coupling between adjacent elements.

The measured results of the reflection coefficient, shown in Figure 8(c), show a minor deviation from the simulated results. Firstly, the return loss has increased from earlier -40 dB for S_{33} to -27 dB. Similarly, the return loss for S_{11}, S_{22} & S_{44} has also increased although the values are still acceptable. Secondly, there is slight shift in resonant frequency range for all four antennas. Antenna-1 now has -10 dB bandwidth ranging from 27.46 to 28.44 GHz, Antenna-2 ranging from 27.48 to 28.39 GHz, Antenna-3 ranging from 27.46 to 28.42 GHz, and Antenna-4 ranging from 27.46 to 28.44 GHz. Although we can clearly see that in all four cases, the n261 range (27.5 to 28.35 GHz) gets completely covered.

The measured results for mutual coupling also show slight deviation. The mutual isolation which was less than -20 dB in simulated results is now measured to be less than -18.5 dB. The deviation in the measured and simulated results can be due to the addition of connectors and cables losses and measuring environment errors. Since the dimensions of the structure are very small, slight variation can cause deviation in characteristics. Additionally, the design required precise alignment of the feed plane and ground plane. However, the measured results of the prototype are still well within the acceptable values.

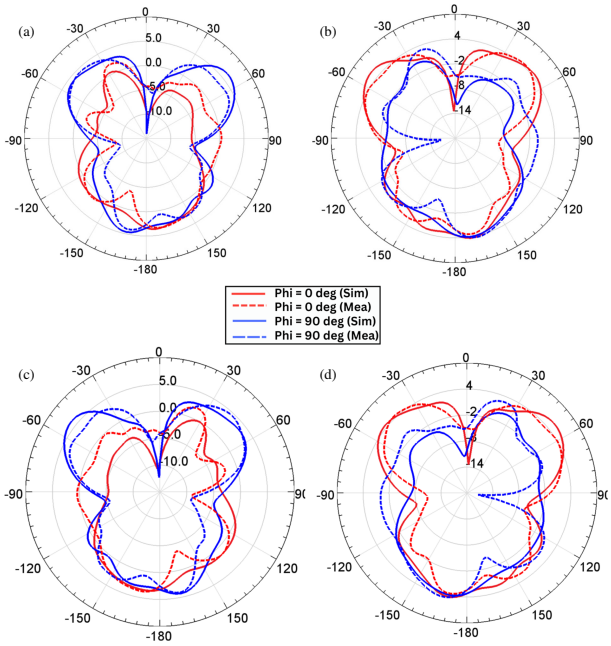

FIGURE 9. Radiation characteristics (dB). (a) Antenna-1. (b) Antenna-2. (c) Antenna-3. (d) Antenna-4.

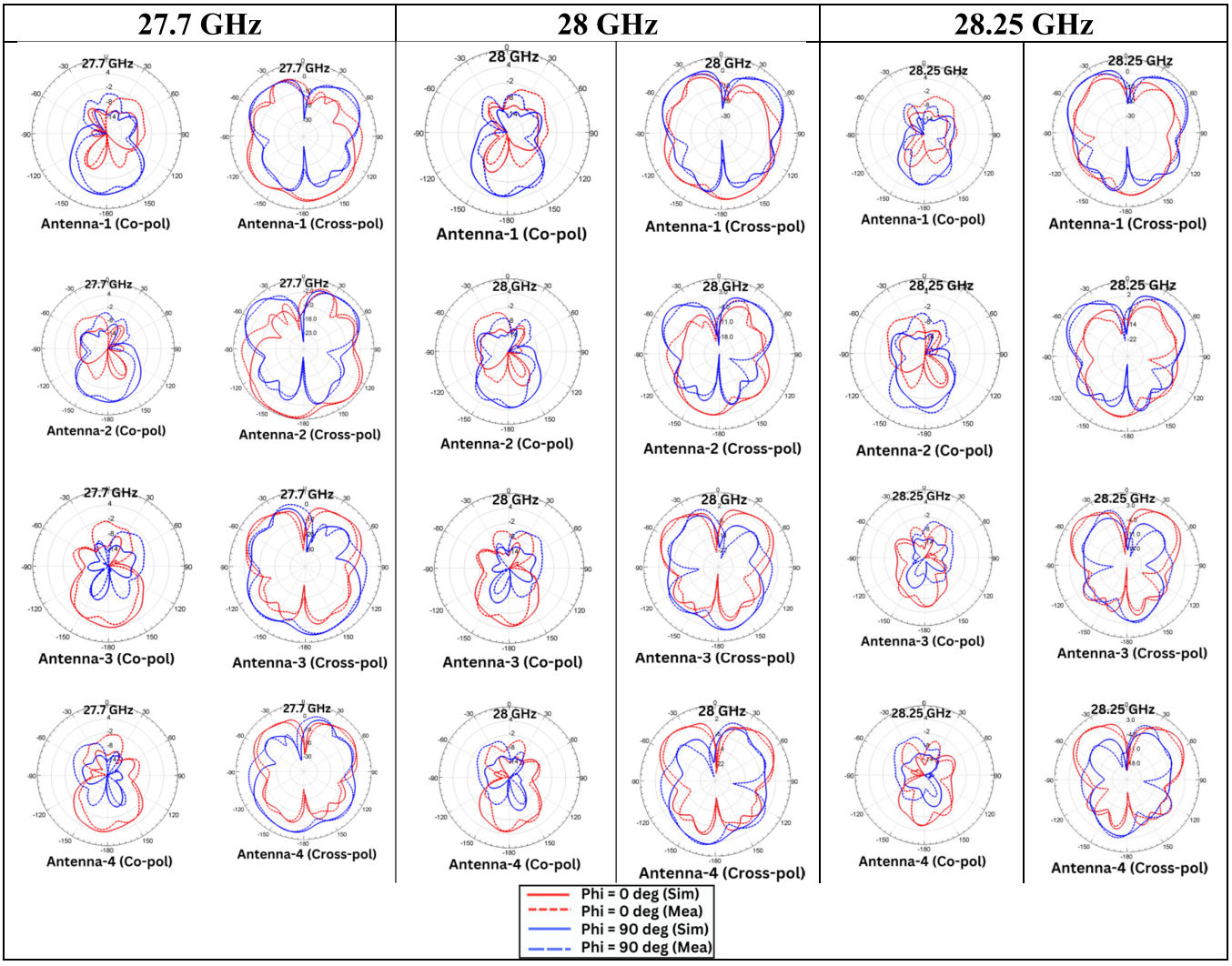

FIGURE 10. Radiation characteristics (dB) at 28 GHz, 27.7 GHz, and 28.25 GHz.

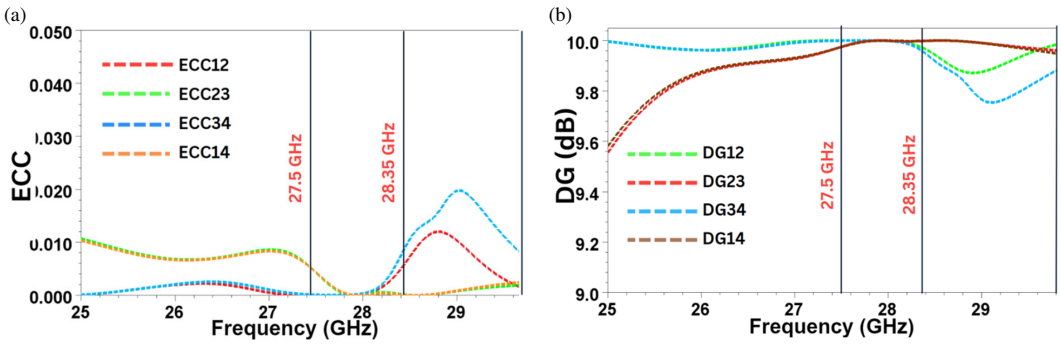

FIGURE 11. (a) Envelop Correlation Coefficient (ECC). (b) Diversity Gain (DG).

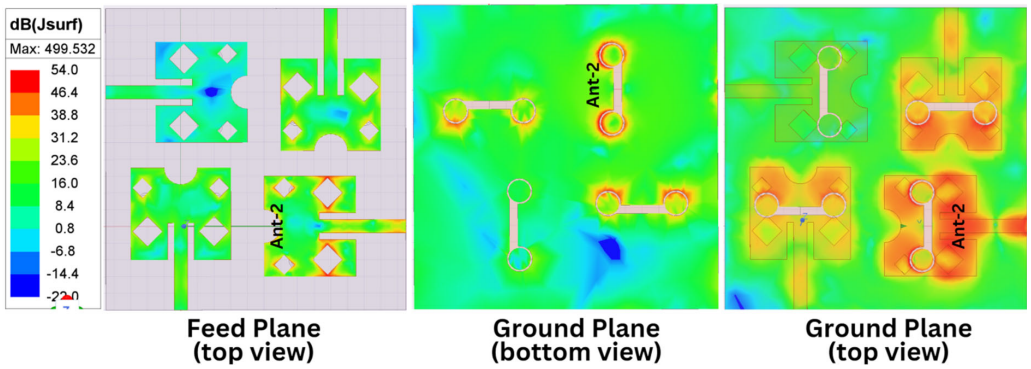

FIGURE 12. Surface current for Antenna-2 at 27.8 GHz.

6.2. Radiation Characteristics

The measured and simulated results of far-field radiation pattern of the proposed 4-element MIMO antenna are as shown in Figures 9(a)–(d). The radiation pattern is captured by keeping the frequency at 28 GHz. The gain characteristics of each antenna are presented for $= 0°$ and $= 90°$. The radiation patterns of antenna-1 & 3 and antenna-2 & 4 are seen as mirror image with each other and their main lobe in reverse order as compared with its corresponding antenna. This is because radiating elements of MIMO antennas are placed perpendicular to each other.

In addition, the radiation patterns of co-polarizations and cross-polarizations are shown in Figure 10. The radiation patterns have been taken at three frequencies for all four antennas, respectively. One observation is taken approximately at the middle of the bandwidth range, which is 28 GHz. Other two observations are taken at the edge of the frequency range, which are 27.7 GHz and 28.25 GHz.

6.3. MIMO Parameters

In MIMO antenna design, diversity parameters play a vital role to determine MIMO performance. Among these parameters, diversity gain (DG), envelop correlation coefficient (ECC), and mean effective gain (MEG) are important. ECC is used to determine the extent to which the MIMO antenna elements are isolated. Ideally the value of ECC should be near zero, but in practical applications values less than 0.5 are considered acceptable. The value of ECC for MIMO antenna can be calculated from S-parameters using the formula below [23]

$$\text{ECC} = \frac{|Sjj * Sji + Sij * Sii|^2}{\left(1 - |Sjj|^2 - |Sji|^2\right)\left(1 - |Sij|^2 - |Sii|^2\right)}$$

where Sii & Sjj are reflection coefficients, and Sji & Sij are the transmission coefficients.

We can see from Figure 11(a) that the simulated ECC value is less than 0.011 in the desired frequency band of n261.

The diversity gain (DG) is calculated using the formula mentioned in [24] as stated below

$$\text{DG} = 10\sqrt{(1 - \text{ECC}^2)}$$

As shown in Figure 11(b), the value attained for DG is greater than 9.90 dB.

6.4. Surface Current

Induced surface current at 28.8 GHz for one antenna (Antenna-2) is shown in Figure 12. As can be seen, large current is induced in dumbbell-shaped slot in ground plane. This is in line with our earlier discussion in Section 4 where we notice significant change in resonant frequency when radius of the circular slot of dumbbell is changed. Also, the width of the horizontal rod of dumbbell was changed, and there was large variation in resonant frequency. So, we can clearly infer that the dumbbell-shaped slot in ground plane has significant role to play in achieving antenna response. Surface current for only

one antenna is shown as other antennas also follow a similar pattern.

Table 1 shows the comparison of earlier published articles related to four port MIMO structures with the proposed structures.

7. CONCLUSION

In this paper, we have furnished a narrowband antenna covering specifically n261 band with range 27.5 GHz to 28.35 GHz with a bandwidth of 850 MHz. Firstly, we have described the characteristics of single element antenna, and later it has been extended to a 4-port MIMO antenna. The overall structural dimensions achieved for proposed 4-port MIMO antenna are $20 \times 19 \times 0.254\,\text{mm}^3$ which to the best of the knowledge of authors are smaller than other structures proposed in literature for this band. Additionally, the proposed antenna is narrowband typically covering only n261 band meant for applications requiring the use of this specific band. ECC is less than 0.011, and DG is greater than 9.90 dB in the mentioned band, which are within tolerance limits. The isolation between neighbouring MIMO elements is also less than -19.5 dB in n261 band.

REFERENCES

[1] Khandelwal, M. K., B. K. Kanaujia, and S. Kumar, "Defected ground structure: Fundamentals, analysis, and applications in modern wireless trends," *International Journal of Antennas and Propagation*, Vol. 2017, No. 1, 2018527, 2017.

[2] Rahman, S., X.-C. Ren, A. Altaf, M. Irfan, M. Abdullah, F. Muhammad, M. R. Anjum, S. N. F. Mursal, and F. S. AlKahtani, "Nature inspired MIMO antenna system for future mmWave technologies," *Micromachines*, Vol. 11, No. 12, 1083, 2020.

[3] Khalid, M., S. I. Naqvi, N. Hussain, M. Rahman, Fawad, S. S. Mirjavadi, M. J. Khan, and Y. Amin, "4-port MIMO antenna with defected ground structure for 5G millimeter wave applications," *Electronics*, Vol. 9, No. 1, 71, 2020.

[4] Bilal, M., S. I. Naqvi, N. Hussain, Y. Amin, and N. Kim, "High-isolation MIMO antenna for 5G millimeter-wave communication systems," *Electronics*, Vol. 11, No. 6, 962, 2022.

[5] Wei, F., Q. Y. Wu, X. W. Shi, and L. Chen, "Compact UWB bandpass filter with dual notched bands based on SCRLH resonator," *IEEE Microwave and Wireless Components Letters*, Vol. 21, No. 1, 28–30, Jan. 2011.

[6] Wei, F., L. Xu, X.-W. Shi, and B. Liu, "Compact UWB bandpass filter with two notch bands based on folded SIR," *Electronics Letters*, Vol. 46, No. 25, 1679–1680, Dec. 2010.

[7] Ebrahimi, A., T. Baum, and K. Ghorbani, "Differential bandpass filters based on dumbbell-shaped defected ground resonators," *IEEE Microwave and Wireless Components Letters*, Vol. 28, No. 2, 129–131, 2018.

[8] Safwat, A. M. E., F. Podevin, P. Ferrari, and A. Vilcot, "Tunable bandstop defected ground structure resonator using reconfigurable dumbbell-shaped coplanar waveguide," *IEEE Trans. on Microw. Theory and Techn.*, Vol. 54, No. 9, 3559–3564, 2006.

[9] Su, L., J. Muñoz-Enano, P. Vélez, J. Martel, F. Medina, and F. Martí, "On the modeling of microstrip lines loaded with dumbbell defect-ground-structure (DB-DGS) and folded DB-DGS resonators," *IEEE Access*, Vol. 9, 150 878–150 888, 2021.

[10] Rehman, S. U., A. F. Sheta, and M. Alkanhal, "Compact band-stop filter using defected ground structure (DGS)," in *2011 Saudi International Electronics, Communications and Photonics Conference (SIECPC)*, 1–4, Riyadh, Saudi Arabia, Apr. 2011.

[11] Vélez, P., J. Muñoz-Enano, M. Gil, J. Mata-Contreras, and F. Martín, "Differential microfluidic sensors based on dumbbell-shaped defect ground structures in microstrip technology: Analysis, optimization, and applications," *Sensors*, Vol. 19, No. 14, 3189, 2019.

[12] Liu, W.-T., C.-H. Tsai, T.-W. Han, and T.-L. Wu, "An embedded common-mode suppression filter for GHz differential signals using periodic defected ground plane," *IEEE Microwave and Wireless Components Letters*, Vol. 18, No. 4, 248–250, Apr. 2008.

[13] Palepu, N. R., J. Kumar, S. Peddakrishna, and A. Ghosh, "Wideband meander-line-antipodal-Vivaldi slot-antenna for millimeter-wave applications," *e-Prime - Advances in Electrical Engineering, Electronics and Energy*, Vol. 9, 100641, 2024.

[14] Gupta, A., M. Kumari, M. Sharma, M. H. Alsharif, P. Uthansakul, M. Uthansakul, and S. Bansal, "8-port MIMO antenna at 27 GHz for n261 band and exploring for body centric communication," *PloS One*, Vol. 19, No. 6, e0305524, 2024.

[15] Sharma, M., P. R. Kapula, S. Salagrama, K. Sharma, G. P. Pandey, D. K. Singh, M. Mahajan, and A. Gupta, "Miniaturized quad-port conformal multi-band (QPC-MB) MIMO antenna for on-body wireless systems in microwave-millimeter bands," *IEEE Access*, Vol. 11, 105 982–105 999, 2023.

[16] Sim, C.-Y.-D., J.-J. Lo, and Z. N. Chen, "Design of a broadband millimeter-wave array antenna for 5G applications," *IEEE Antennas and Wireless Propagation Letters*, Vol. 22, No. 5, 1030–1034, May 2023.

[17] Hussain, N., W. A. Awan, W. Ali, S. I. Naqvi, A. Zaidi, and T. T. Le, "Compact wideband patch antenna and its MIMO configuration for 28 GHz applications," *AEU — International Journal of Electronics and Communications*, Vol. 132, 153612, 2021.

[18] Balanis, C. A., *Antenna Theory: Analysis and Design*, 4th ed., John Wiley & Sons, Hoboken, New Jersey, 2016.

[19] Pozar, D. M., *Microwave Engineering*, 3rd ed., John Wiley & Sons, Hoboken, New Jersey, 2009.

[20] Murthy, N., "Improved isolation metamaterial inspired mm-Wave MIMO dielectric resonator antenna for 5G application," *Progress In Electromagnetics Research C*, Vol. 100, 247–261, 2020.

[21] Sharawi, M. S., S. K. Podilchak, M. T. Hussain, and Y. M. M. Antar, "Dielectric resonator based MIMO antenna system enabling millimetre-wave mobile devices," *IET Microwaves, Antennas & Propagation*, Vol. 11, No. 2, 287–293, 2017.

[22] Kamal, M. M., S. Yang, X.-C. Ren, A. Altaf, S. H. Kiani, M. R. Anjum, A. Iqbal, M. Asif, and S. I. Saeed, "Infinity shell shaped MIMO antenna array for mm-Wave 5G applications," *Electronics*, Vol. 10, No. 2, 165, 2021.

[23] Mazloum, J., S. A. Ghorashi, M. Ojaroudi, and N. Ojaroudi, "Compact triple-band S-shaped monopole diversity antenna for MIMO applications," *The Applied Computational Electromagnetics Society Journal (ACES)*, Vol. 30, No. 9, 975–980, 2015.

[24] Kumar, A., A. Q. Ansari, B. K. Kanaujia, and J. Kishor, "High isolation compact four-port MIMO antenna loaded with CSRR for multiband applications," *Frequenz*, Vol. 72, No. 9-10, 415–427, 2018.